energies

MDPI

Article

# Model for the Discharging of a Dual PCM Heat Storage Tank and Its Experimental Validation

**Artur Nemś [1,*] and Antonio M. Puertas [2,3]**

1 Department of Thermodynamics and Renewable Energy Sources, Wroclaw University of Science and Technology, Wybrzeże Wyspiańskiego 27, 50-370 Wroclaw, Poland
2 Dpto. de Química y Física, Universidad de Almería, 04120 Almería, Spain; apuertas@ual.es
3 CIESOL, Joint Center University of Almería-CIEMAT, 04120 Almería, Spain
* Correspondence: artur.nems@pwr.edu.pl; Tel.: +48-71-320-36-73

Received: 16 September 2020; Accepted: 28 October 2020; Published: 30 October 2020


**Abstract:** The important topic of modelling tanks filled with phase change materials (PCMs) is discussed in this article. Due to the increasing use of heating and cooling installations, tanks containing two types of PCMs are the subject of many experimental analyses. However, there are still deficiencies in their models, which are presented in this paper. The theory model was created in order to design two tanks, each with a volume of 2 $m^3$. They were filled with water and containers with two PCMs. The modelled tanks were meant to replace the existing water tanks that were previously used in the solar heating and cooling installation in a research building located in the southern part of Spain. After the tanks were assembled, the model was validated during the summer period when the designed storage tanks supported the operation of the solar system operating in the cooling mode. The created model consists of a 1D description of the heat transfer in the storage tank, and also a 1D description of the phase change in the containers with the PCMs. The model takes into account the front of the phase change and also discusses its impact on the thermal efficiency of the tanks. The agreement of the water output temperature is very good and validates the model, which can then be used to provide further details on the operation of the storage system—in particular, heat fluxes or a fraction of solid or liquid PCM.

**Keywords:** thermal storage; phase change materials; heat transfer process

## 1. Introduction

Thermal storage in phase change materials is currently the subject of many studies regarding materials science, thermodynamics and engineering. The good storage properties of PCMs contribute to their common application in various areas of life. The most frequently mentioned is the accumulation of both heat and cold in domestic hot water tanks in order to increase the amount of accumulated energy and to increase the thermal comfort of buildings integrated with PCMs. This is achieved through free cooling and heating passive methods [1], or free cooling active methods [2]. The desire to achieve a high density of energy storage is associated with a series of works in which one of the end effects is the cooperation of heat storage with the heating and cooling installation [3]. When necessary, two tanks with PCMs for the storing of heat and cold are used, which work for the purpose of a heat pump [4] or a sorption chiller [5]. Experimental studies are the final result of many research works. However, information about the operation of an accumulator is required at the design stage. Therefore, mathematical models describing the heat storage process are created using various techniques. In studies on the impact of the application of PCM that is integrated with a building, EnergyPlus software can be used. This was the case with the authors of the paper [6], who examined the energy efficiency of a building and then verified their model experimentally.

In the case of thermal energy storage (TES) in PCMs, the descriptions of heat transfer during the melting and solidification processes are the basic problems that determine the efficiency of these systems. The heat transfer mechanism has not yet been sufficiently well investigated and understood [7], and therefore various techniques are used to accurately imitate this process. In the literature, there are many models for the simulation of the heat storage process, which describe it with different degrees of accuracy. Some of them concern the thermal properties of a material, such as the one described in [8], which was a modification of the generally known model of storing heat in a sensible and latent form in PCM. This model corrects the amount of stored heat by changing the characteristic of specific heat C(T). Many more studies concern the operation of the entire tank with PCM, in which commercial codes are used. This is the case in [9], where a new component of the TRNSYS program was developed in order to simulate the operation of a water tank with cylindrical packages filled with PCM. The calculation algorithm used in this component did not take into account the heat transfer on the side of the PCM and the changing thermal resistance on the side of the PCM, which resulted from the moving front of the phase change. TRNSYS software was also used to compare the cooperation of a solar heating and cooling system with tanks filled with various PCMs and a tank filled with water [10]. The research described in [11] showed a numerical model of a rectangular tank filled with spheres with two types of PCMs for heating and cooling. This model was created in the commercial STAR-CCM+ program. The influence of the proportion between the cooling-PCM and heating-PCM on the speed of the tank's discharging process was investigated. In the model, the authors used the effective thermal conductivity, but did not take into account the thermal resistance of the sphere and the heat losses to the environment. Moreover, the model was only verified on a small scale with regards to heating demands, and concerned only the heating-PCM. In [12], the authors used the commercial Comsol software in order to develop a 2D model of a cylindrical tank filled with PCM spheres. In their model, three different types of PCMs were used in order to improve the efficiency of high-temperature storage. The authors ignored the heat losses from the surface of the tank, even though the temperature of the fluid in the tank was between 250 and 400 °C. What is more, they assumed that the temperature of the fluid was constant. They used a phase change function $\alpha$ as a parameter that determines the parameters during the phase change, but the influence of this parameter on the heat transfer flux was not sufficiently explained. More complex models were created using CFD programs, as is the case in [13], where the authors used a heat exchange model in a tank with cylindrical packets filled with PCM. This was a 2D model, and in order to speed up the calculations, the convective heat transfer on the side of the PCM, and also its thermal conductivity, were omitted. In turn, [14] showed a model of a heat tank created using Ansys Fluent software. This model concerns the heat transfer between the PCM, which is enclosed in spheres, and the water flowing around them. Due to the duration of single calculations, it did not provide much information about the operation of the entire heat accumulator.

In paper [15], the authors presented an extensive 3D model of a sphere filled with PCM. They investigated the effect of the pins mounted inside a sphere, and also the effect of a copper-plated sphere with 32 internally built copper pins. Due to the conducted validation, this model could be used for further optimization of TES tanks filled with spherical encapsulated PCM.

There are also many other models in the literature that describe the charging process of a tank. They are usually 0, 1 or 2D models. The 0D models are not complicated, but provide a lot of information about the cooperation of the heat accumulator with the installation. Paper [16] presented a simple method of modelling the efficiency of a thermal energy storage system that uses PCM. The 0D model was created for both the water tank and the PCM package, and did not include a heat exchanger - heat is transferred immediately. As the authors themselves emphasized, the proposed method is particularly suitable for applications at the initial stages of designing, as it does not provide results with high accuracy. In turn, in [17], the authors used a simplified model of a PCM tank in order to determine the optimal operating parameters of a solar cooling installation. The model divided the calculations into two stages: the first one describing the heat transfer when the PCM was in the solid phase, and the second one when it was melting. Simplifications concerned, among others, the scope of

calculations, which only took into account the PCM cylinders located in the center of the tank, and the constant heat transfer coefficient on the side of the water. Article [18] also described a 2D model of a tank containing cylindrical packages filled with PCM. The model does not include the convective heat transfer from the side of the PCM. In turn, in paper [19], the authors presented a model of heat transfer in a tank containing PCM, which cooperated with a cooling device. This model included a detailed description of the heat exchange process between the water and the PCM. However, the results of their experiment were used to describe the convective heat exchange in the liquid phase of the PCM. In paper [20], the authors presented a model of a tank filled with spheres with three different high-temperature PCMs. They showed an advanced model of heat exchange between the air and the PCMs. The authors used the correlation concerning the effective thermal conductivity coefficient for the PCM, but the method of implementing this relationship in the model was not clearly presented. The authors obtained a high compatibility with the results of the experiment, despite the fact that the model ignored the heat losses to the environment and that the air flowing through the tank had a temperature of 350–550 °C.

There are many models in the literature in which significant simplifications were applied, such as the omission of the occurrence of convection inside the PCM, the neglect of the thermal resistance of the casing in which the storage material was enclosed [21], or the omission of the thermal resistance of the PCM during both the phase change and after solidification [22]. Paper [23] presents a model of a tank filled with PCM packages. This model used a third order polynomial to describe the heat transfer coefficient. An installation consisting of three high-efficient ammonia chillers/heat pumps and four PCM cold storage tanks of about 60 $m^3$ each was used for the validation of the model. A detailed analysis of the simulation results is presented in [24]. Different assumptions were made in [25], in which the authors assumed that the heat transfer coefficient through the cylindrical container, regardless of the water flow rate and the temperature of the PCM, has a constant value. Moreover, the temperature of the cylinder was assumed to be the same as the temperature of the PCM. There are also models that use experimental data, e.g., to describe the heat transfer coefficient, as presented in [26]. However, this solution is only possible when using the results of an already running installation.

The authors of paper [27] presented a heat exchange model for a building partition in which two PCMs with different phase transition temperatures were used. This model was experimentally validated in test cells, where free convection occurred on both sides of the wall, and heat was transferred between the partition and the air. Another dual PCM model that uses the enthalpy method was described in [28]. This work includes extensive analysis for various materials, but the simulation results have not yet been experimentally verified. The dual PCM model was also described in [29]. This article presented the results of the simulation of a high-temperature heat tank, in which one of the materials is a metal that changes its state of aggregation. Another area of research in which two types of PCMs were used was described in [30]. There, experimental results of a flat-plate solar collector in which two PCMs are used to protect against overheating and freezing are presented.

Many models in the literature were prepared for the implementation of specific tasks, e.g., to better understand the heat transfer process and the flow of the material filling a storage tank, to determine the change of initial parameters in a tank, or to simulate the cooperation of a storage tank with a heat source or a receiver. The authors found one model, described in [11], which takes into account the work of a tank filled with PCMs for heat and cold storage. That model contained a number of simplifications, and the performed validation was incomplete. Therefore, in the present work, a model of a tank filled with two types of PCMs is presented. This modelling served to design two tanks that were installed in a research building in southern Spain. This allowed the model to be validated with experimental results.

## 2. Methods

The work described in this article was carried out as part of the European PCMSOL project. The project aims to develop new materials for thermal storage in the form of latent heat and implement

them in an actual facility. It includes the modelling of PCM containers and storage tanks, and also the analysis of the performance of the tanks. A detailed description of the overall work that was carried out within the project can be found in [31]. The designed PCM tanks were meant to be incorporated into the existing solar heating and cooling installation in the CIESOL building—the center for research concerning solar energy—located in the University of Almeria in Spain. Before the beginning of the works, this installation used two water tanks with a total capacity of 5 $m^3$. The other elements included: flat solar collectors for obtaining the hot water that drives the LiBr-H2O absorption chiller with a rated capacity of 70 kW; a cooling tower; a shallow geothermal heat dissipation system; two hot water tanks; and additional devices, as shown in Figure 1. A more detailed description of the system's operation can be found in [32–34].

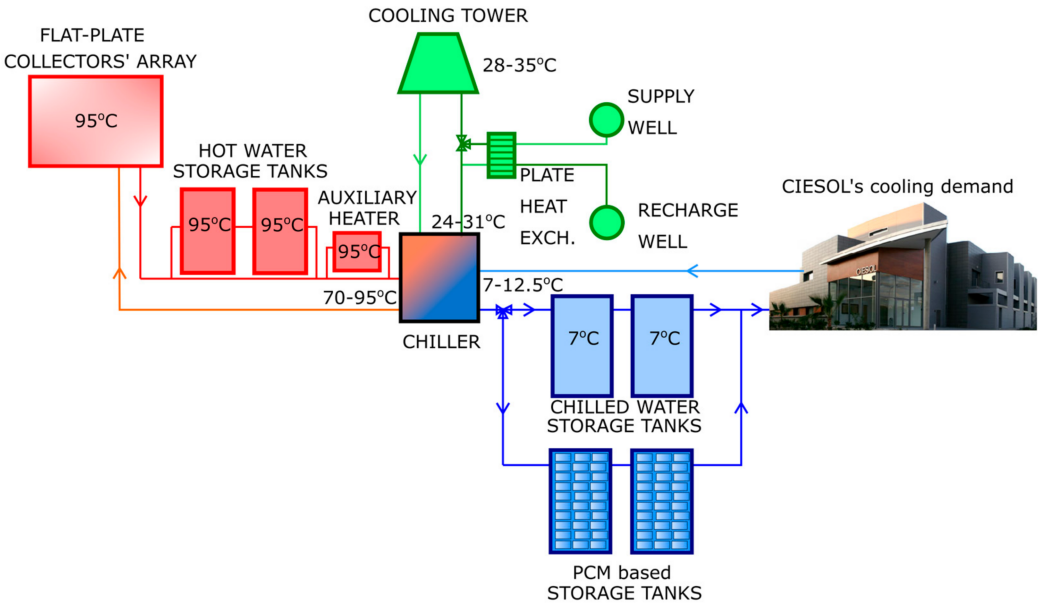


**Figure 1.** The heating and cooling installation of the CIESOL building (Almeria), using storage tanks with phase change materials (PCMs) or chilled water.

*Description of the Heat Transfer Model*

Works on the model began with the determination of the requirements for the tanks with PCMs. The data recorded during the operation of the solar heating and cooling installation with the water tanks allowed the capacity of the designed tanks with the PCMs to be determined. Two $m^3$ tanks were selected. The project assumed that these tanks would be used to store heat and cold. Due to the meteorological conditions of Almeria, the heating and cooling installation covers the heating demands for 3 months of the year and cooling demand for 5 months. As was shown in the experimental tests [32] that were carried out on the discussed installation, in order to ensure the required thermal comfort in the heating mode, the temperature of the water that supplies the building is between 40 and 45 °C, and in the summer period, when the system operates in the cooling mode, the water temperature is usually from 7 to 15 °C.

Based on the observations, it was decided that the phase transition temperature of the PCM for storing cold should be around 10 °C, and for heat storage it should be slightly higher than 45 °C. Therefore, two commercial PCMs from PCMProducts, S10 and S46, were selected. They are characterized by a phase change temperature equal to ca. 10 and 46 °C, respectively. Some relevant parameters of the selected materials are presented in Table 1.

**Table 1.** Parameters of the selected phase change materials as provided by the supplier.

| PCM | Phase Change Temperature | Density | Latent Heat Capacity | Specific Heat Capacity | Thermal Conductivity | Max. Operating Temperature |
|---|---|---|---|---|---|---|
| | °C | kg/m$^3$ | kJ/kg | kJ/(kg·K) | W/(m·K) | °C |
| S10 | 10 | 1.470 | 155 | 1.90 | 0.43 | 60 |
| S46 | 46 | 1.587 | 210 | 2.41 | 0.45 | 56 |

PCM containers, which are offered by the supplier of the S10 and S46 materials, were also selected, i.e., ICEFlat containers with outer dimensions of 0.500 × 0.250 × 0.032 m and a thickness of approximately 3 mm. By arranging 4 containers in a horizontal layer, it was possible to place 198 containers in each of the tanks. It was assumed that they would be arranged in a staggered manner so that the flow was as turbulent as possible. Both tanks had similar internal distributions of both PCM containers, i.e., every tank contained a mixture of both containers. Therefore, in the process of heating the building, the S10 material accumulated heat in a sensible form. The number of containers filled with the S10 and S46 materials was important. Thus, at the design stage, it was decided to check the different proportions (see Table 2) of these substances.

**Table 2.** The number of containers with the used PCMs as a function of their share in a 2000 L tank.

| PCM\Proportions | 50–50% | 40–60% | 30–70% | 20–80% | 15–85% | 12–88% | 10–90% |
|---|---|---|---|---|---|---|---|
| S46 | 99 | 79 | 59 | 40 | 30 | 24 | 20 |
| S10 | 99 | 119 | 139 | 158 | 168 | 174 | 178 |

Due to the high insolation in this area, the cooling demands are about three times higher than the heating demands [35]. Therefore, one of the basic tasks of the created model was to determine the proportion of the PCMs for storing heat and cold. The greater share of PCMs for the cold storage was caused by the much greater demand for cooling in the building. The results of the preliminary simulations, which were described in [36], show that the proportions should be close to 15–85%. Therefore, additional analyses were performed, and 24 containers containing S46, and 174 filled with S10, were selected. Two tanks were then built with an internal height $l_{tank}$ of 2.065 m, an internal diameter $d_{tank}$ of 1.100 m, and an insulation thickness $\delta_{ins}$ of 0.100 m. The tanks were filled with the PCMs for heating and cooling and then incorporated into the installation that covers the thermal demands of the CIESOL building.

An important issue in the operation of tanks with PCMs is the time during which they will cover the cooling demands of the building. The longer they run, the less frequently the chiller will start, and the system will in turn run more efficiently [31]. Therefore, simulations of the discharging of the tanks were the main subject of the design work concerning the tanks.

It was assumed that the heat transfer model should be as accurate as possible in order to correctly reflect the thermal processes that take place in the tanks. At the same time, it could not be a model that would make a wide case analysis difficult, as there were many variables to be checked at the design stage. That is why 2D or 3D CFD models were discarded. Instead, it was decided to describe the thermal processes in several heat transfer equations that can be solved in a simple calculation program.

The model takes into account the heat exchange between the flowing water and the PCM containers, and also the heat losses of the tank. Furthermore, the dependence of the temperature with the vertical position in the tank will be considered, i.e., the model will be 1D. The process parameters will change with the flow of water in the tanks. In addition, the 1D model was also used in the description of the phase change process that occurs inside the PCM containers. It was assumed that the heat exchange process takes place only through the two largest surfaces of the selected containers. This means that the phase change in the tank's discharge process occurs from the wall of the container to its center. The other assumptions made in the model are as follows:

– the thermal conductivity of storage tanks' insulation is 0.034 W/(m·K),
– the convective heat transfer coefficient on the PCM side is replaced by thermal conductivity for the liquid and solid phase (described below),
– the ICEFlat container heat transfer coefficient equals 13 W/(m·K).

The thermal model for the tanks was described for only one of them, because the other was identical. The scheme of the tank, with the designation of the material and process parameters, is shown in Figure 2. It should be noted that the model takes into account heat losses to the environment, which include heat absorbed by the tank in the cooling mode. The heat loss flux is small when compared to the heat exchanged between the water and the PCM in the first minutes of discharging. However, when this flux decreases over time, heat losses are noticeable. Therefore, the general balance Equation (1), which compares the heat flux supplied by the water flowing through the tank $\dot{Q}_{water}$ and the heat losses $\dot{Q}_{loss}$ with the heat absorbed by the material S10 $\dot{Q}_{cold}$ and S46 $\dot{Q}_{hot}$, should be written as:

$$\dot{Q}_{water} + \dot{Q}_{loss} = \dot{Q}_{cold} + \dot{Q}_{hot} \tag{1}$$

The heat flux supplied by flowing water $\dot{Q}_{water}$ can be written as (2).

$$\dot{Q}_{water} = \dot{m}_{water} \cdot Cp_{water} (T_{water\_inlet} - T_{water\_outlet}) \tag{2}$$

The heat loss flux $\dot{Q}_{loss}$(3) is the sum of the losses from the top surface $\dot{Q}_{loss\_top}$, the bottom surface $\dot{Q}_{loss\_bot}$, and the side surface $\dot{Q}_{loss\_side}$, namely:

$$\dot{Q}_{loss} = \dot{Q}_{loss\_top} + \dot{Q}_{loss\_bot} + \dot{Q}_{loss\_side} \tag{3}$$

The heat flux passing through each of the tank's surfaces takes into account the process of free convection and radiation on the side of the environment, the thermal conductivity of the insulation, and the forced convection on the inside. The thermal resistance of the material of which the tank's walls are made is neglected due to their small thickness and high thermal conductivity coefficient. Therefore, the heat flux from the side surface is given by Equation (4).

$$\dot{Q}_{loss\_side} = \frac{T_{amb} - T_{water\_avg}}{\frac{1}{h_{con\_side\_in}} + \frac{ln\left(\frac{D_{tank}}{d_{tank}}\right)}{2\pi\lambda_{ins}} + \frac{1}{h_{con\_side\_out} + h_{rad\_side\_out}}} (l_{tank} + \delta_{ins}) \tag{4}$$

The average water temperature $T_{water\_avg}$ is calculated as the arithmetic mean of the inlet water temperature and the outlet water temperature from the calculation area. The bottom and top surfaces of the tank are flat, and therefore the heat loss flux formulas for these surfaces are almost the same—written as (5) and (6).

$$\dot{Q}_{loss\_top} = \frac{T_{amb} - T_{water\_avg}}{\frac{1}{h_{con\_top\_in}} + \frac{\delta_{ins}}{\lambda_{ins}} + \frac{1}{h_{con\_top\_out} + h_{rad\_top\_out}}} [\pi \frac{(d_{tank} + \delta_{ins})^2}{4}] \tag{5}$$

$$\dot{Q}_{loss\_bot} = \frac{T_{amb} - T_{water_{avg}}}{\frac{1}{h_{con\_bot\_in}} + \frac{\delta_{ins}}{\lambda_{ins}} + \frac{1}{h_{con\_bot\_out} + h_{rad\_bot\_out}}} [\pi \frac{(d_{tank} + \delta_{ins})^2}{4}] \tag{6}$$

The convective heat transfer coefficient on the outer side of the wall is described by Equation (7).

$$h_{con\_i\_out} = \frac{\lambda_{air} \cdot Nu_{i\_out}}{x} \tag{7}$$

The dimension that is characteristic for the top and bottom surfaces is the outer diameter of the tank $D_{tank}$, and for the lateral surface, it is the outer height $L_{tank}$. It should be added that this

coefficient was increased by 30% for the top surface, and correspondingly decreased by 30% for the bottom surface. This is due to the direction of the fluid movement that is caused by the difference in air density. The Nusselt number in this case is written using general Equation (8) [37].

$$Nu_{i\_out} = \mathrm{A}(\mathrm{Gr}\cdot\mathrm{Pr})^{B} \tag{8}$$

Constants A and B in Equation (8) depend on the product Gr · Pr and take the values [37]:

$$\left\{ \begin{array}{c} \mathrm{A} = 0.5,\ \mathrm{B} = 0\ if\ \mathrm{Gr}\cdot\mathrm{Pr} < 10^{-3} \\ \mathrm{A} = 1.18,\ \mathrm{B} = 1/8\ if\ 10^{-3} \le \mathrm{Gr}\cdot\mathrm{Pr} < 500 \\ \mathrm{A} = 0.54,\ \mathrm{B} = 1/4\ if\ 500 \le \mathrm{Gr}\cdot\mathrm{Pr} < 2\cdot 10^{7} \\ \mathrm{A} = 0.135,\ \mathrm{B} = 1/3\ if\ 2\cdot 10^{7} \le \mathrm{Gr}\cdot\mathrm{Pr} \end{array} \right\}$$

The Grashof number is described using Equation (9), where the characteristic parameter is the same as in the convective heat transfer coefficient.

$$\mathrm{Gr}_{i\_out} = \frac{g\cdot x^{3}\cdot\beta\cdot\Delta T_{i\_out}}{{\nu_{air}}^{2}} \tag{9}$$

The temperature difference $\Delta T_{i\_out}$, as indicated in Figure 2, for the top, bottom and side surfaces is described as $T_{amb} - T_{top\_out}$, $T_{amb} - T_{bot\_out}$ and $T_{amb} - T_{side\_out}$, respectively.

For the radiative heat transfer coefficient on the outer side of the tank, Equation (10) was used.

$$h_{rad\_i\_out} = \frac{\varepsilon_{out}\cdot\sigma\cdot\left({T_{amb}}^{4} - {T_{i\_out}}^{4}\right)}{T_{amb} - T_{i\_out}} \tag{10}$$

The heat transfer coefficient on the inside of the tank for each of the surfaces $h_{con\_i\_in}$ is calculated from Equation (7), substituting the thermal conductivity of water and the Nusselt number that is calculated for the respective surface. The characteristic dimensions, similar to the convection on the outer side, are the inner diameter and the height of the tank. The Nusselt number for the cylindrical wall inside the tank is determined from (11) [37],

$$Nu_{side\_in} = 1.86\left(\frac{\frac{\dot{m}_{water}}{\mathrm{A}_{real}}\cdot x}{\nu_{water}}\cdot\frac{l_{tank}}{d_{tank}}\right)^{0.33}\cdot\mathrm{Pr}^{0.25} \tag{11}$$

whereas for a horizontal flat wall, the Nusselt number is determined from (12).

$$Nu_{i\cdot in} = 0.664\left(\frac{\frac{\dot{m}_{water}}{\mathrm{A}_{real}}\cdot x}{\nu_{water}}\right)^{0.5}\cdot\mathrm{Pr}^{0.33} \tag{12}$$

The characteristic dimensions x are the same as for $h_{con\_i\_in}$, and the actual cross-sectional area of the tank $\mathrm{A}_{real}$ is calculated from Equation (13), taking into account the area occupied by the PCM containers.

$$\mathrm{A}_{real} = \frac{\pi\frac{{d_{tank}}^{4}}{4}}{l_{tank}} - 4a_{ICEFlat}\cdot b_{ICEFlat} \tag{13}$$

The part of the tank's model that is responsible for describing the heat exchange process between the flowing water and the PCM has two components, which describe the heat transfer between the water and S10, and the water and S46. The differences result from the phase change in the S10, which means there is movement of the phase change front from which the heat is transferred to the center of the container. It should be noted that in the cooling mode, there is no phase change in the S46 material. The heat released by the S46 material comes from the heat stored in the form of specific heat. Due to

the fact that the S46 is in the solid phase throughout the entire process, it was assumed that heat is transferred by conduction from the entire volume of the material in the container, and that the thermal resistance from the entire volume is calculated for half of the distance between the container's wall to its center.

The process parameters change as the tank is discharged. The PCM's temperature is a suitable parameter for controlling the heat transfer process when the material is not undergoing a phase change. However, when the transformation takes place at a constant temperature, it is necessary to enter the enthalpy as a process control parameter. In the presented model, the enthalpy of the phase change was replaced by an increased specific heat in a narrow range of temperatures around the melting point, which is denoted as $\Delta h_{S10}$. For the S10, it was found that the heat varies linearly between 10 and 11 °C.

The heat flux that is transferred between the water and the S10 is described by (14). It takes into account the variable thermal resistance during the phase change.

$$\dot{Q}_{cold} = \begin{cases} \frac{n_{S10} \cdot \frac{S_{ICEFlat\_in} + S_{ICEFlat\_out}}{2} \left(T_{water\_avg} - T_{S10\_f}\right)}{\frac{1}{h_{water\_S10}} + \frac{\delta_{ICEFlat}}{\lambda_{ICEFlat}} + \frac{\frac{c_{ICEFlat}}{4}}{\lambda_{S10}}}, T_{S10\_f} \geq T_{S10\_s} \\ \frac{n_{S10} \cdot \frac{S_{ICEFlat\_in} + S_{ICEFlat\_out}}{2} \left(T_{water\_avg} - T_{S10\_f}\right)}{\frac{1}{h_{water\_S10}} + \frac{\delta_{ICEFlat}}{\lambda_{ICEFlat}} + \frac{\frac{c_{ICEFlat}}{2} \cdot S}{\lambda_{S10}}}, T_{S10\_s} > T_{S10\_f} > T_{S10\_m} \\ \frac{n_{S10} \cdot \frac{S_{ICEFlat\_in} + S_{ICEFlat\_out}}{2} \left(T_{water\_avg} - T_{S10\_f}\right)}{\frac{1}{h_{water\_S10}} + \frac{\delta_{ICEFlat}}{\lambda_{ICEFlat}} + \frac{\frac{c_{ICEFlat}}{4}}{\lambda_{S10}}}, T_{S10\_m} \geq T_{S10\_f} \end{cases} \quad (14)$$

Parameter S was defined as the front of the phase change and is specified as the distance from which the heat in the S10 is released from the wall of the ICEFlat container (marked in Figure 2). It is described by Equation (15).

$$S = \frac{T_{S10\_f} - T_{S10\_m}}{T_{S10\_s} - T_{S10\_m}} \quad (15)$$

The heat flux that is transferred between the water and the S10 is equal to the heat flux that is stored in the S10 (16),

$$\dot{Q}_{cold} = \begin{cases} \frac{(nmCp)_{S10} \cdot (T_{S10\_m} - T_{S10\_0}) + n_{S10} \cdot m_{S10} \cdot h_{S10} + (nmCp)_{S10} \cdot \left(T_{S10\_f} - T_{S10\_s}\right)}{\tau}, T_{S10\_f} \geq T_{S10\_s} \\ \frac{(nmCp)_{S10} \cdot (T_{S10\_m} - T_{S10\_0}) + n_{S10} \cdot 2\left(a_{ICEFlat} \cdot b_{ICEFlat} \cdot \frac{c_{ICEFlat}}{2} \cdot S\right) \cdot \rho_{S10} \cdot h_{S10}}{\tau}, T_{S10\_s} > T_{S10\_f} > T_{S10\_m} \\ \frac{(nmCp)_{S10} \cdot \left(T_{S10\_f} - T_{S10\_0}\right)}{\tau}, T_{S10\_m} \geq T_{S10\_f} \end{cases} \quad (16)$$

where $(nmCp)_{S10}$ means $n_{S10} \cdot m_{S10} \cdot Cp_{S10}$. and $\tau$ is the time step for the numerical integration.

The heat exchanged between the water and the S46 is described by (17).

$$\dot{Q}_{hot} = \frac{n_{S46} \cdot \frac{S_{ICEFlat\_in} + S_{ICEFlat\_out}}{2} \left(T_{water\_avg} - T_{S46\_f}\right)}{\frac{1}{h_{water\_S46}} + \frac{\delta_{ICEFlat}}{\lambda_{ICEFlat}} + \frac{\frac{c_{ICEFlat}}{4}}{\lambda_{S46}}} \quad (17)$$

This flux is stored by the S46 in the form of sensible heat (18).

$$\dot{Q}_{hot} = \frac{n_{S46} \cdot m_{S46} \cdot Cp_{S46} \cdot \left(T_{S46\_f} - T_{S46\_0}\right)}{\tau} \quad (18)$$

The heat transfer coefficient on the side of the water $h_{water\_S}$ is described by Equation (7), to which the thermal conductivity of the water is substituted. The characteristic dimension is the width of the container $b_{ICEFlat}$, and the Nusselt number is calculated as in Equation (12).

The above equations allow the process parameters, the temperature of the water flowing from the tank, and the PCM temperature to be determined.

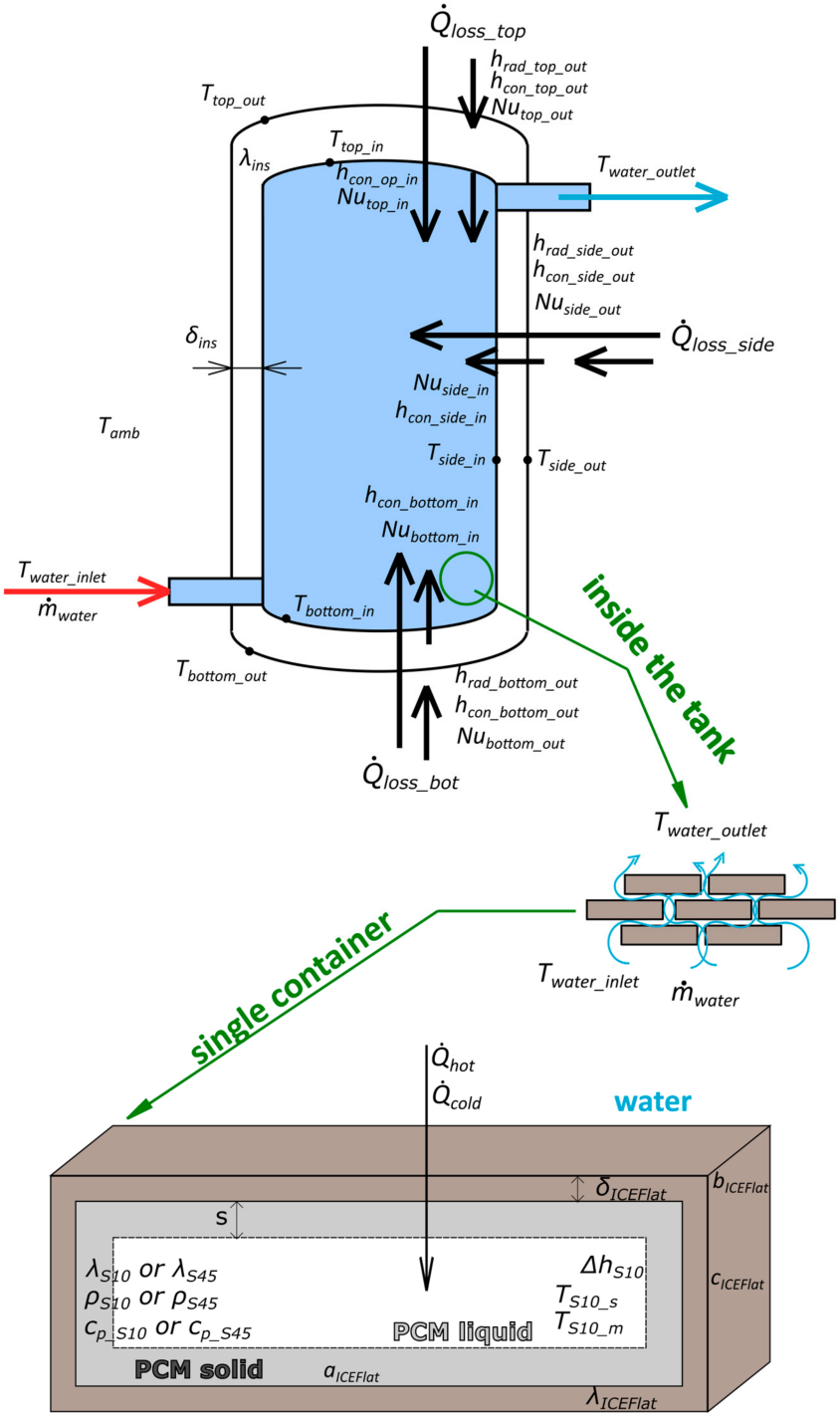


**Figure 2.** Scheme of the PCM storage tank with marked physical parameters describing the thermal balance.

## 3. Model Validation

The model encoded in the set of differential equations described above was solved numerically. The calculations were made using Mathcad 15. As mentioned earlier, the simulation predictions were described in a previous paper [36]. Therefore, this section contains the validation of the model using

the experimental data from the operating installation. These data include the temperature of the water entering and leaving the tanks, the water flow rate, and the temperature of the water inside the tanks. The following assumptions for the model were introduced on the basis of the experimental data:

- the tanks operate in a cascade configuration, which means that the first tank is discharged first. When the temperature of outflowing water reaches 15 °C, the water flow is redirected into tank 2, and the temperature of water outflowing from tank 1 is the same as the temperature of water flowing into tank 2,
- the initial temperature of the PCMs in both tanks, according to the sensors located in the tanks, is equal to 6.5 °C,
- the ambient temperature is equal to 25.0 °C,
- the water flow rate is 7 $m^3$/h,
- the temperature of the water flowing into the tank is taken from the experiment and is shown in Figure 3.

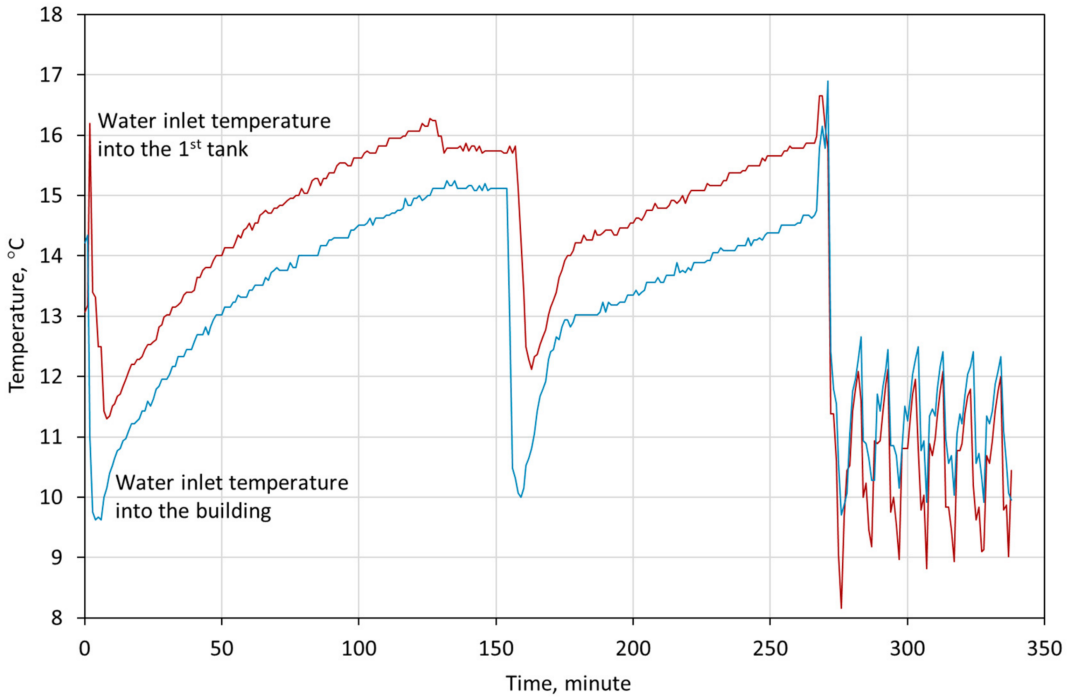


**Figure 3.** The results of measuring the temperature of the water entering and leaving the tanks during their discharge for the system operating in the cascade mode.

The studies, the results of which are shown in Figure 3, were made in September 2019. The tanks were charged and left in order to obtain steady state conditions. Afterwards, during the operation of the cooling system, the chiller was turned off and the system was switched to the tanks. The process of switching on the first tank is shown in Figure 3 as the characteristic water temperature jump in the first minutes of the measurements. The temperature of the water flowing through the tank increased, and when it reached a temperature of 15 °C, the control system switched the second tank into the cooling circuit and the tanks began to work in the series mode. The tests ended when the temperature of the water flowing from the second tank reached the maximum allowable temperature. After this time, the tanks were disconnected and the chiller was started. This device works cyclically, which is shown by the frequent changes in temperature on the right side of the graph.

The model includes all the material parameters of the tanks and the PCMs: the initial temperature of the PCMs, which is based on the measured temperature of the water inside the tanks after a long time of stagnation, and the temperature of the water entering the tanks, which changes over time.

The model was validated on the basis of the temperature of water flowing out of the tanks, because this is the control parameter for the operation of the cooling system, and also because this is a value that is determined in the mathematical model. Figure 4 shows the temperature of the water flowing out of the tanks, which was recorded during the experimental tests, and also that obtained from the model.

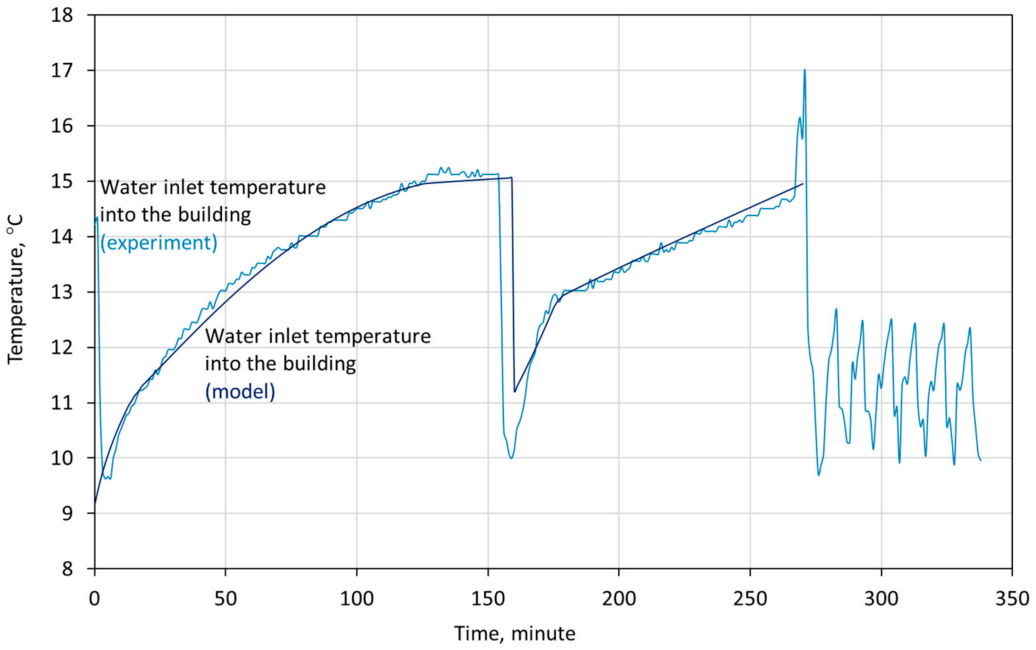


**Figure 4.** Comparison of the temperature of water flowing from the tanks in the process of cooling the building.

The results show a high compatibility with the change in water temperature over time, as the model curve corresponds to the empirical results. Moreover, the differences in temperature values are small; they are noticeable when attaching the second tank to the system. There may be two factors that have an influence on this. The first is that the model provides an immediate response to the changing inlet temperature. In the experimental tests, the tanks have a capacity of 2 $m^3$ each. This means that there is inertia due to the time the water flows through the tanks. The second reason may be the inlet water temperature, which changes with the building's cooling demands. This change is visible in the time preceding the attachment of the second tank. This does not change the fact that the model reflects changes in water temperature and responds correctly to the input parameters.

## 4. Discussion

When assuming that the model is compatible with the experimental data, it is possible to obtain additional information about the modelled process, the obtaining of which is experimentally difficult. The created model provides data including the share of each phase of the material that changes its state of aggregation, the PCMs' temperature, the heat flux, heat losses, heat transfer coefficients, and other factors. At the stage of designing the tanks, two parameters were important: the temperature of the water flowing out of the tanks, and the heat transfer flux between the water and the PCMs. The first one determined the configuration of the cooling system's operation, because it was a control parameter. The second one allowed for the determination of whether the thermal power of the tanks is sufficient to ensure thermal comfort in the building. The results of the research show that the temperature of the water flowing into the tanks increases. Figure 5 shows the change in the power of the tanks during their discharging.

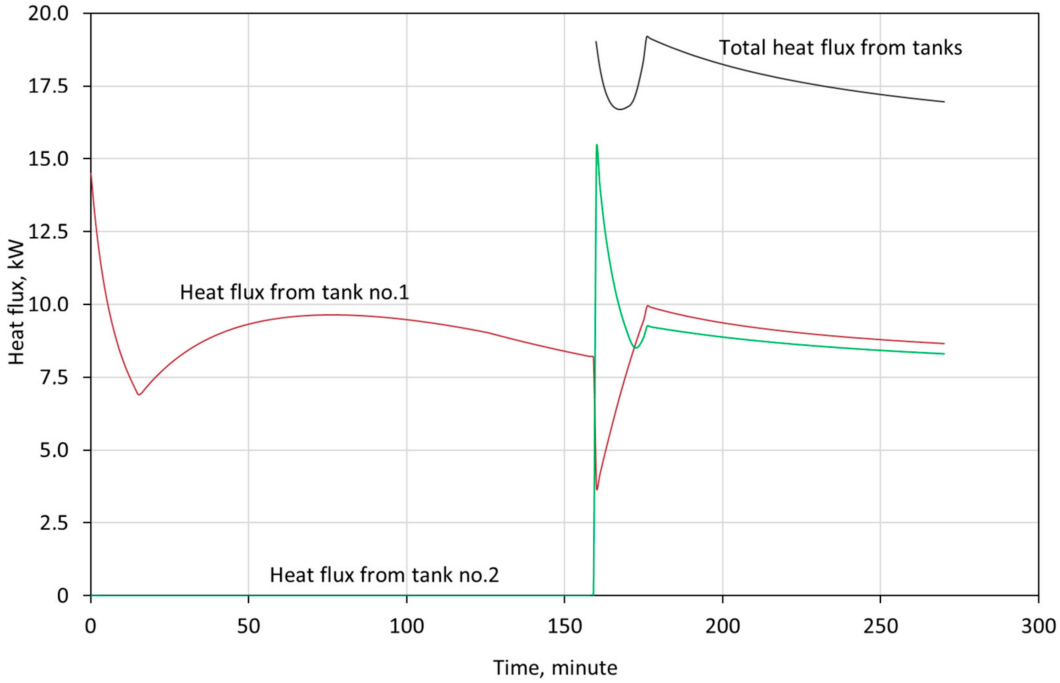


**Figure 5.** The heat flux transferred between the water and the PCMs in the storage tanks during their discharge.

The graph shows a clear decrease in power during the first minutes of the process. The power then increases slightly, which may be due to the increasing temperature of the water entering the tanks. This causes a greater temperature difference between the water and the PCMs. Afterwards, this flux decreases, which, according to Equation (14), may be caused by either the decreasing temperature difference between the water and the PCMs, or by the increasing thermal resistance. Figure 5 shows that the heat flux changes in a similar way after the second tank is connected. Therefore, when analyzing the process, the temperature of the PCMs should be checked.

The average temperatures in the tanks are shown in Figure 6. They show that the temperature of the S46 follows the temperature change of the water flowing through the tanks. However, for the S10, there is deceleration visible in the temperature at which the material melts. This corresponds with a changing flux of transferred heat. When the S10 reached the melting point, the difference between the water and PCM temperatures stopped decreasing. This resulted in a slight increase in the heat transfer flux. However, this flux began to decrease again, which may have been the result of the increasing thermal resistance between the phase change front and the water, and the slightly changing temperature of the S10.

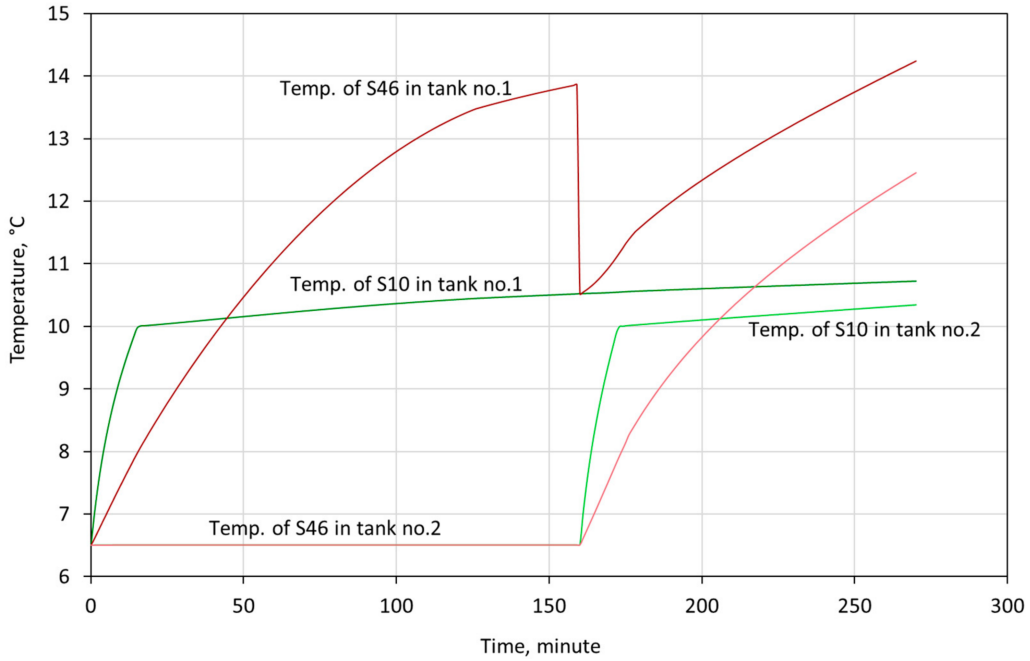


**Figure 6.** Average temperature of the PCMs in the storage tanks during their discharge.

One more parameter that is determined by the model and which provides information about the process is the mass fraction of the liquid phase of the S10. Figure 7 shows the average values for the tanks during their discharging.

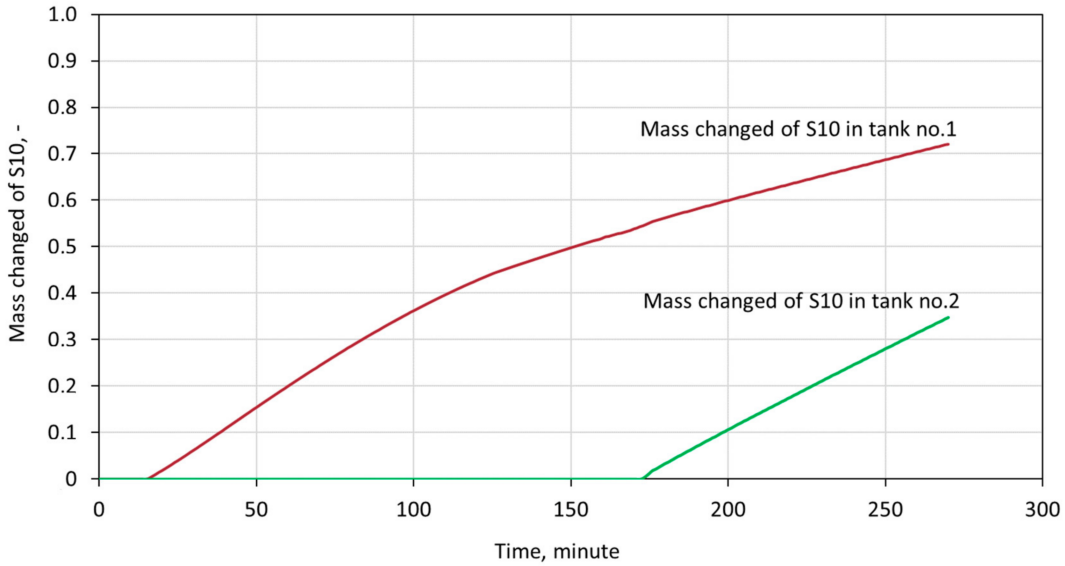


**Figure 7.** Mass fraction of the liquid phase of the S10 in the storage tanks during their discharge.

As can be seen from the diagram, the S10 did not completely melt, either in the first container or in the second one. The increasing amount of the S10 liquid phase means that the phase change front is moving away from the wall of the container. The thermal resistance then increases, in turn causing heat transfer problems. These results show that a significant fraction of the energy stored in the PCM is not recovered during the discharging. Therefore, the settings of the parameters in the experiment should be refined in order to improve the efficiency of the storing system. The mass flow of water

through the tanks has a great influence on the process of heat transfer between the water and the PCM. Therefore, it is possible to intensify the heat transfer by changing the water flow rate.

## 5. Conclusions

There are models available in the literature that describe in approximate ways the process of heat storage in tanks containing PCMs. The authors propose a compromise model that would combine the accuracy of the results with the speed of performing single simulations. However, among the 1D and 2D models in the literature, the authors did not find a model that is suitable for the PCM tanks that they analyzed.

When creating the model, classical heat transfer equations were used in order to describe thermal processes. The problem with the description of convective heat exchange in the PCM was solved by replacing the convective heat transfer coefficient with an effective heat conduction coefficient, which varies with the change of the phase change front. Moreover, the enthalpy of the transition was substituted by the increased specific heat in a narrow temperature range. It allowed the one parameter (the temperature of the PCM that was changing the phase) that controls the heat exchange process to be obtained. This significantly simplified and accelerated the calculation process.

The model was useful at the design stage, but it was also used when collecting data during the operation of the heating and cooling system. In the experimental tests, there is a response of the system to the input parameters of the water entering the building. This information then forms the input impulse for the model. Thanks to this, additional data are obtained from the model, which complement the parameters that were measured during the operation of the installation, and help in the description of the processes that takes place.

The model is not only dedicated to the installation discussed in the paper, but can also be easily adapted to the modelling of similar tanks. Material parameters and geometries can be changed, making the model more universal.

**Author Contributions:** Conceptualization, A.N. and A.M.P.; methodology, A.N.; software, A.N.; validation, A.N. and A.M.P.; formal analysis, A.N.; investigation, A.N.; resources, A.M.P.; data curation, A.M.P.; writing—original draft preparation, A.N.; writing—review and editing, A.N. All authors have read and agreed to the published version of the manuscript.

**Funding:** The financial support for this work was provided by the Polish National Centre for Research and Development (Ref. EraNet-LAC/PCMSOL/08/2017), under the international program ERA-Net LAC, project PCMSOL. The financial support for this work was provided under the ERA-Net LAC, project ELAC2015/T06-0988, PCMSOL. The Spanish team was funded by the Spanish Ministerio de Economía, Industria y Competitividad, project PCIN-2016-013, PCMSOL.

**Conflicts of Interest:** The authors declare no conflict of interest.

## References

1. Ramakrishnan, S.; Sanjayan, J.; Wang, X. Experimental research on using form-stable PCM-integrated cementitious composite for reducing overheating in buildings. *Buildings* **2019**, *9*, 57. [CrossRef]
2. Iten, M.; Liu, S.; Shukla, A. A review on the air-PCM-TES application for free cooling and heating in the buildings. *Renew. Sustain. Energy Rev.* **2016**, *61*, 175–186. [CrossRef]
3. Beaudin, M.; Zareipour, H. A Review of PCM Energy Storage Technology Used in Buildings for the Global Warming Solution. In *Energy Solutions to Combat Global Warming*; Springer: Cham, Switzerland, 2017; Volume 33, ISBN 978-3-319-26948-1.
4. Real, A.; García, V.; Domenech, L.; Renau, J.; Montés, N.; Sánchez, F. Improvement of a heat pump based HVAC system with PCM thermal storage for cold accumulation and heat dissipation. *Energy Build.* **2014**, *83*, 108–116. [CrossRef]
5. Behi, M.; Mirmohammadi, S.A.; Ghanbarpour, M.; Behi, H.; Palm, B. Evaluation of a novel solar driven sorption cooling/heating system integrated with PCM storage compartment. *Energy* **2018**, *164*, 449–464. [CrossRef]

6. Ramakrishnan, S.; Wang, X.; Sanjayan, J.; Wilson, J. Experimental and Numerical Study on Energy Performance of Buildings Integrated with Phase Change Materials. *Energy Procedia* **2017**, *105*, 2214–2219. [CrossRef]
7. Kong, L.B.; Li, T.; Hng, H.H.; Boey, F.; Zhang, T.; Li, S. Preface. In *Waste Energy Harvesting*; Lecture Notes in Energy Series; Springer: Berlin/Heidelberg, Germany, 2014; Volume 24, ISBN 9783642546341.
8. Bakoń, T.; Obstawski, P.; Kozikowska, A. Modelling of Heat Storage Using Phase Change Material Tank. In *Renewable Energy Sources: Engineering, Technology, Innovation*; Springer: Cham, Switzerland, 2020; pp. 809–816. [CrossRef]
9. Ibáñez, M.; Cabeza, L.F.; Solé, C.; Roca, J.; Nogués, M. Modelization of a water tank including a PCM module. *Appl. Therm. Eng.* **2006**, *26*, 1328–1333. [CrossRef]
10. Noro, M.; Lazzarin, R.M.; Busato, F. Solar cooling and heating plants: An energy and economic analysis of liquid sensible vs phase change material (PCM) heat storage. *Int. J. Refrig.* **2014**, *39*, 104–116. [CrossRef]
11. Lee, Y.T.; Kim, M.H.; Lee, S.S.; Gim, J.; Chung, J.D. Numerical analysis in a full-scale thermal energy storage tank with dual PCM capsules. *Energy Build.* **2019**, *204*, 109410. [CrossRef]
12. Mohammadnejad, F.; Hossainpour, S. A CFD modeling and investigation of a packed bed of high temperature phase change materials (PCMs) with different layer configurations. *J. Energy Storage* **2020**, *28*, 101209. [CrossRef]
13. Bourne, S.; Novoselac, A. Compact PCM-based thermal stores for shifting peak cooling loads. *Build. Simul.* **2015**, *8*, 673–688. [CrossRef]
14. Wang, Z.; Zhang, H.; Dou, B.; Zhang, G.; Wu, W. Influence of inlet structure on thermal stratification in a heat storage tank with PCMs: CFD and experimental study. *Appl. Therm. Eng.* **2019**, *162*. [CrossRef]
15. Aziz, S.; Amin, N.A.M.; Abdul Majid, M.S.; Belusko, M.; Bruno, F. CFD simulation of a TES tank comprising a PCM encapsulated in sphere with heat transfer enhancement. *Appl. Therm. Eng.* **2018**, *143*, 1085–1092. [CrossRef]
16. Belmonte, J.F.; Eguía, P.; Molina, A.E.; Almendros-Ibáñez, J.A.; Salgado, R. A simplified method for modeling the thermal performance of storage tanks containing PCMs. *Appl. Therm. Eng.* **2016**, *95*, 394–410. [CrossRef]
17. Gallego, A.J.; Ruíz-Pardo, A.; Cerezuela-Parish, A.; Sánchez, J.; Martín-Macareno, C.; Cabeza, L.F.; Camacho, E.F.; Oró, E. Mathematical modeling of a PCM storage tank in a solar cooling plant. *Sol. Energy* **2013**, *93*, 1–10. [CrossRef]
18. Lin, W.; Ma, Z.; McDowell, C.; Baghi, Y.; Banfield, B. Optimal design of a thermal energy storage system using phase change materials for a net-zero energy Solar Decathlon house. *Energy Build.* **2020**, *208*, 109626. [CrossRef]
19. Barragan-Cervera, Á.; Domenech, L.; Fernando, S.; Maiorino, A.; Aprea, C. Modeling of a PCM TES Tank Used as an Alternative Heat Sink for a Water Chiller. Analysis of Performance and Energy Savings. *Energies* **2019**, *12*, 3652.
20. Carmona, M.; Rincón, A.; Gulfo, L. Energy and exergy model with parametric study of a hot water storage tank with PCM for domestic applications and experimental validation for multiple operational scenarios. *Energy Convers. Manag.* **2020**, *222*, 113189. [CrossRef]
21. Roccamena, L.; El Mankibi, M.; Stathopoulos, N. Development and validation of the numerical model of an innovative PCM based thermal storage system. *J. Energy Storage* **2019**, *24*, 100740. [CrossRef]
22. Raul, A.; Jain, M.; Gaikwad, S.; Saha, S.K. Modelling and experimental study of latent heat thermal energy storage with encapsulated PCMs for solar thermal applications. *Appl. Therm. Eng.* **2018**, *143*, 415–428. [CrossRef]
23. Jokiel, M.; Kauko, H.; Schlemminger, C.; Hafner, A.; Claussen, I.C. Phase change material thermal energy storage for a large ammonia chiller/heat pump system. In Proceedings of the 7th Conference on Ammonia and CO2 Refrigeration Technology, Ohrid, Macedonia, 11–13 May 2017; pp. 179–186. [CrossRef]
24. Jokiel, M. *Development and Performance Analysis of an Object-Oriented Model for Phase Change Material Thermal Storage*; Project Work; SINTEF Energy Research: Trondheim, Norway, 2016.
25. Mousa, H.; Naser, J.; Houche, O. Using PCM as energy storage material in water tanks: Theoretical and experimental investigation. *J. Energy Storage* **2019**, *22*, 1–7. [CrossRef]
26. Abdelsalam, M.Y.; Teamah, H.M.; Lightstone, M.F.; Cotton, J.S. Hybrid thermal energy storage with phase change materials for solar domestic hot water applications: Direct versus indirect heat exchange systems. *Renew. Energy* **2020**, *147*, 77–88. [CrossRef]

27. Singh, S.P.; Bhat, V. Performance evaluation of dual phase change material gypsum board for the reduction of temperature swings in a building prototype in composite climate. *Energy Build.* **2018**, *159*, 191–200. [CrossRef]
28. Lakhdari, Y.A.; Chikh, S.; Campo, A. Analysis of the thermal response of a dual phase change material embedded in a multi-layered building envelope. *Appl. Therm. Eng.* **2020**, *179*, 115502. [CrossRef]
29. Wang, G.; Xu, C.; Wei, G.; Du, X. Numerical study of a novel dual-PCM thermal energy storage structure filled with inorganic salts and metal alloy as the PCMs. *Energy Procedia* **2019**, *158*, 4423–4428. [CrossRef]
30. Wang, D.; Liu, H.; Liu, Y.; Xu, T.; Wang, Y.; Du, H.; Wang, X.; Liu, J. Frost and High-temperature resistance performance of a novel dual-phase change material flat plate solar collector. *Sol. Energy Mater. Sol. Cells* **2019**, *201*. [CrossRef]
31. Batlles, F.J.; Gil, B.; Ushak, S.; Kasperski, J.; Luján, M.; Maldonado, D.; Nemś, M.; Nemś, A.; Puertas, A.M.; Romero-Cano, M.S.; et al. Development and Results from Application of PCM-Based Storage Tanks in a Solar Thermal Comfort System of an Institutional Building—A Case Study. *Energies* **2020**, *13*, 3877. [CrossRef]
32. Rosiek, S.; Batlles, F.J. Reducing a solar-assisted air-conditioning system's energy consumption by applying real-time occupancy sensors and chilled water storage tanks throughout the summer: A case study. *Energy Convers. Manag.* **2013**, *76*, 1029–1042. [CrossRef]
33. Rosiek, S.; Batlles, F.J. Renewable energy solutions for building cooling, heating and power system installed in an institutional building: Case study in southern Spain. *Renew. Sustain. Energy Rev.* **2013**, *26*, 147–168. [CrossRef]
34. Rosiek, S.; Batlles Garrido, F.J. Performance evaluation of solar-assisted air-conditioning system with chilled water storage (CIESOL building). *Energy Convers. Manag.* **2012**, *55*, 81–92. [CrossRef]
35. Gil, B.; Rosiek, S.; Kasperski, J.; Nemś, M.; Nemś, A. Analysis of heat gains in a real research building: The difference in the need of air conditioning systems for various locations around the world. In Proceedings of the ECOS 2019—32nd International Conference on Efficiency, Cost, Optimization, Simulation and Environmental Impact of Energy Systems, Wrocław, Poland, 23–28 June 2019; pp. 2559–2570.
36. Nems, A.; Nems, M.; Rosiek, S.; Puertas, A.M.; Gil, B.; Kasperski, J.; Batlles, F.J. Modeling of the discharging process of a heat storage tank filled with PCM to cover the heat demand of a building. In Proceedings of the EA SHC International Conference onSolar Heating and Cooling for Buildings and Industry, Santiago, Chile, 3–7 November 2019; pp. 1393–1404. [CrossRef]
37. Kostowski, E. *Zbiór Zadań z Przepływu Ciepła*; Wydawnictwo Politechniki Śląskiej: Gliwice, Poland, 2006; ISBN 83-88000-18-7.